



Contents lists available at ScienceDirect

Bioorganic & Medicinal Chemistry

journal homepage: www.elsevier.com/locate/bmc

Microbial transformation of glycyrrhetic acid derivatives by *Bacillus subtilis* ATCC 6633 and *Bacillus megaterium* CGMCC 1.1741

Pingping Shen^{a,1}, Jian Zhang^{a,b,1}, Yuyuan Zhu^a, Wei Wang^a, Boyang Yu^b, Weiwei Wang^{a,b,*}

^a State Key Laboratory of Natural Medicines, China Pharmaceutical University, Nanjing 210009, PR China

^b Jiangsu Key Laboratory of TCM Evaluation and Translational Research, School of Traditional Chinese Pharmacy, China Pharmaceutical University, Nanjing 211198, PR China

ARTICLE INFO

Keywords:

Glycyrrhetic acid derivatives
 Pentacyclic triterpene
 Biotransformation
 Glycosylation
 Hydroxylation

ABSTRACT

Glycyrrhetic acid (GA), the major bioactive pentacyclic triterpene aglycone of licorice root, was known to play a vital role in anti-ulcer, anti-depressant, anti-inflammatory, and anti-allergic. In this study, we semi-synthesized five GA derivatives by a series of chemical reactions. They were selected as substrates for the biotransformation and yielded thirteen metabolites by *Bacillus subtilis* ATCC 6633 and *Bacillus megaterium* CGMCC 1.1741. Their structures were identified on the basis of extensive spectroscopic methods and nine of them were found for the first time. Two main types of reactions, regio- and stereo-selective hydroxylation and glycosylation, especially in the unactivated C-H bonds including C-11, C-19 and C-27, were observed in the biotransformation process, which greatly expand the chemical diversities of GA derivatives. All compounds were tested for their inhibitory effects on nitric oxide (NO) generation in lipopolysaccharide (LPS)-stimulated RAW 264.7 cells. Among them, olean-12-ene-3 β ,7 β ,15 α ,19 α ,30-pentol (**16**) and olean-12-ene-3 β ,7 β ,15 α ,27,30-pentol (**17**) showed significant inhibitory effect with IC₅₀ values of 0.64 and 0.07 μ M, respectively.

1. Introduction

Licorice (*Glycyrrhiza*), one of the most widely used herbal medicines, frequently appearing in various prescriptions for the treatment of diseases ranging from cough to peptic ulcers.¹ The major bioactive ingredient in licorice is glycyrrhizin, which is mainly administered in the therapy for hepatitis B and C in Japan.^{2,3} Glycyrrhetic acid (GA, **1**), the aglycone of glycyrrhizin isolated from licorice root, has been reported to possess a variety of biological effects such as anti-inflammatory, antibacterial, anti-depressant, anti-ulcer, anti-allergen, and anti-malarial.^{4,5} However, some undesirable physical-chemical properties of GA, including high hydrophobicity, low water solubility and membrane permeability were observed, which contribute to inadequate bioavailability, and seriously restrict its potential clinical applications.^{6,7} To broaden biological windows, numerous chemical modifications based on the GA framework have been explored. Deoxoglycyrrhetol dihemiphthalate (DGDH) (Fig. 1), disodium phthalate of deoxoglycyrrhetol, have been synthesized and reported to have a remarkable analgesic effect like aspirin through suppression of PGE2 production.^{8,9}

Biotransformation is an alternative chemical tool for the development of sustainable technologies to produce chemicals and drugs of commercial importance because of the abundant variety of enzymes available in microorganisms.¹⁰ In the previous study, more than 100 biotransformation products were obtained from natural pentacyclic terpenoids (PTs), confirming that microbial transformation is an attractive method to expand the chemical diversity of structurally complex natural products.¹¹ With the chemical versatility and a broad substrate range of cytochromes P450, *Bacillus megaterium* was widely served as a biocatalyst for the selective oxidation of various natural products.^{12,13} *Bacillus subtilis*, holding the inherent robust glycosyltransferases, could efficiently catalyze a vast variety of compounds for the synthesis of high-value glycosylation products.¹⁴ In biosynthetic pathways of PTs, a series of site-specific oxidations of the skeleton are involved in the late stages, most probably catalyzed by P450s and followed by glycosylations catalyzed through UDP glycosyltransferases (UGTs). Such modifications are essential for improving their biological activities and physicochemical features.^{15,16} Herein, in continuation of our studies on the biotransformation of bioactive PTs, a series of

* Corresponding author at: Jiangsu Key Laboratory of TCM Evaluation and Translational Research, School of Traditional Chinese Pharmacy, China Pharmaceutical University, Nanjing 211198, PR China.

E-mail addresses: shpp1127@163.com (P. Shen), wilsonzhang99@cpu.edu.cn (J. Zhang), yuyuanzhu616@163.com (Y. Zhu), 1721020352@stu.cpu.edu.cn (W. Wang), weiweiwang@cpu.edu.cn (W. Wang).

¹ Contributed equally to this work.

<https://doi.org/10.1016/j.bmc.2020.115465>

Received 14 January 2020; Received in revised form 18 March 2020; Accepted 22 March 2020

0968-0896/ © 2020 Elsevier Ltd. All rights reserved.

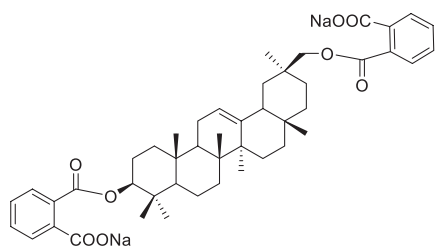


Fig. 1. Structure of deoxoglycyrrhetol dihemiphthalate (DGDH).

synthetic compounds as starting aglycon, we prepared five glycosylated derivatives by *Bacillus subtilis* ATCC 6633 and eight oxidized products by *Bacillus megaterium* CGMCC 1.1741. Among them, nine metabolites were isolated for the first time. All the compounds were evaluated for their anti-inflammatory activity upon nitric oxide (NO) production in lipopolysaccharide (LPS)-induced RAW 264.7 cells.

2. Results and discussion

2.1. Substrates preparation

GA and oleanolic acid were obtained commercially and served as a precursor in the chemical synthesis of five products 2–6 according to the previous procedures (Fig. 2). Firstly, GA was reduced with LiAlH_4 and subsequently oxidated through MnO_2 , to give principal product glycyrrhetol and a small quantity of by-product glycyrrhaldehyde.^{17,18} Secondly, oleanolic acid was used as a lead for the preparation of 11-oxo-oleanolic acid by stepwise chemical reactions (C-3 protection, C-11 oxidation and C-3 deprotection) following the previous study.^{19,20} Furthermore, GA and glycyrrhetol as substrates, through the Clemmenson reduction reaction, two C-11 decarbonylation products 5 and 6 were prepared, respectively.²¹

2.2. Biotransformation

Preparative scale biotransformation, isolation and structure elucidation of purified products were investigated. GA with a free hydroxyl group on C-3 and a carboxyl group on C-30 on the skeleton is easily glycosylated, particularly, C-30 carboxyl group. Microbial

transformation of GA (1, 200 mg) with *B. subtilis* resulted in two known glycosylation products 7 and 8. Compound 7 was obtained as a white powder, possessing a $[\text{M}+\text{H}]^+$ ion at m/z 633.3966 (calcd for $\text{C}_{36}\text{H}_{57}\text{O}_9$, 633.3997), indicating a 162 amu mass increase to that of compound 1. Compound 8 was isolated as a white powder, giving a $[\text{M}+\text{Cl}]^-$ ion at m/z 829.4158 (calcd for $\text{C}_{42}\text{H}_{66}\text{O}_{14}\text{Cl}$, 829.4147) in the HR-ESI-MS, indicating a 162 amu mass increase to that of 7. By comparison of the spectroscopic data in the literature,²² their structures were elucidated as 30-O- β -D-glucopyranosyl glycyrrhetinic acid and 3-O-(β -D-glucopyranosyl) glycyrrhetinic acid-30-O- β -D-glucopyranoside (Fig. 3).

Incubation of glycyrrhaldehyde (2, 200 mg) with *B. subtilis* led to the production of compound 9. It was isolated as a white powder, gave a $[\text{M}+\text{Cl}]^-$ ion at m/z 651.4124 (calcd for $\text{C}_{36}\text{H}_{56}\text{O}_8\text{Cl}$, 651.3669) in the HR-ESI-MS, indicating a 162 amu mass increase to that of 2. By contrast with the ^1D NMR spectrum data of 2, compound 9 was elucidated as 30-O- β -D-glucopyranosyl glycyrrhaldehyde (Fig. 3).

Fermentation of glycyrrhetol (3, 200 mg) with *B. subtilis* resulted in one new glycosylated product 10. It was obtained as a white powder, gave a $[\text{M}+\text{H}]^+$ ion at m/z 619.4232 (calcd for $\text{C}_{36}\text{H}_{59}\text{O}_8$, 619.4204) in the HR-ESI-MS, indicating a 162 amu mass increase to that of 3. By further contrast with the ^{13}C NMR spectrum of 3, compound 10 was elucidated as 3-O-(β -D-glucopyranosyl) glycyrrhetol (Fig. 3).

Treating 11-oxo-oleanolic acid (4, 200 mg) with *B. subtilis* obtained one known mono-glycosylated metabolite 11. Compound 11, isolated as a white powder, gave a $[\text{M}+\text{H}]^+$ ion at m/z 633.4012 (calcd for $\text{C}_{36}\text{H}_{57}\text{O}_9$, 633.3997) in the HR-ESI-MS, indicating a 162 amu mass increase to that of compound 4. By comparing its ^{13}C NMR spectrum with those reported in the literature, compound 11 was elucidated as 11-oxo-oleanolic acid-28-O- β -D-glucopyranoside (Fig. 3).

Incubation of 11-deoxoglycyrrhetinic acid (5, 200 mg) with *B. megaterium* obtained one new hydroxylated product 12. Its structure was elucidated as 3 β ,7 β ,27-trihydroxy-olean-12-ene-30-oic acid on the basis of HR-ESI-MS and NMR spectrum (Fig. 4).

Compound 12, isolated as a white powder, gave a $[\text{M}+\text{Cl}]^-$ ion at m/z 523.3179 (calcd for $\text{C}_{30}\text{H}_{48}\text{O}_5\text{Cl}$, 523.3196) in the HR-ESI-MS, indicating a 32 amu mass increase to that of compound 5. The ^{13}C NMR spectrum showed the presence of one new methine carbon signal at δ 74.3 ppm. And the new proton signal δ 4.66 (1H, dd, $J = 10.9, 4.6$ Hz) ppm showed the direct ^1H - ^{13}C correlation with δ 74.3 ppm in HSQC

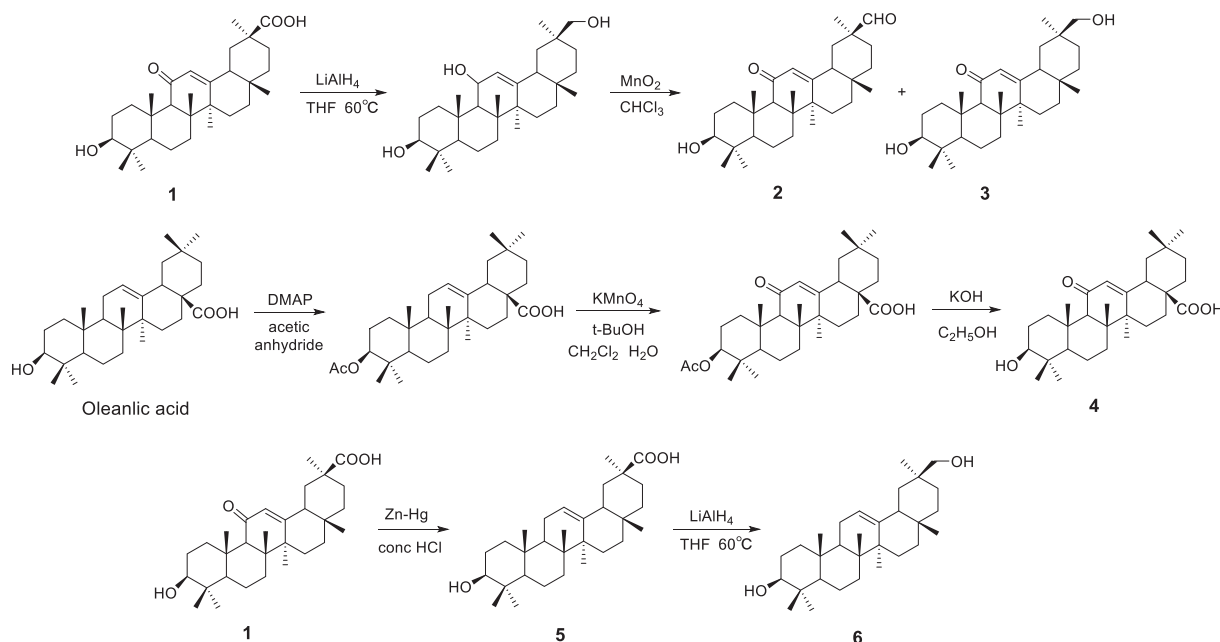


Fig. 2. Synthetic routes of compounds 2–6.

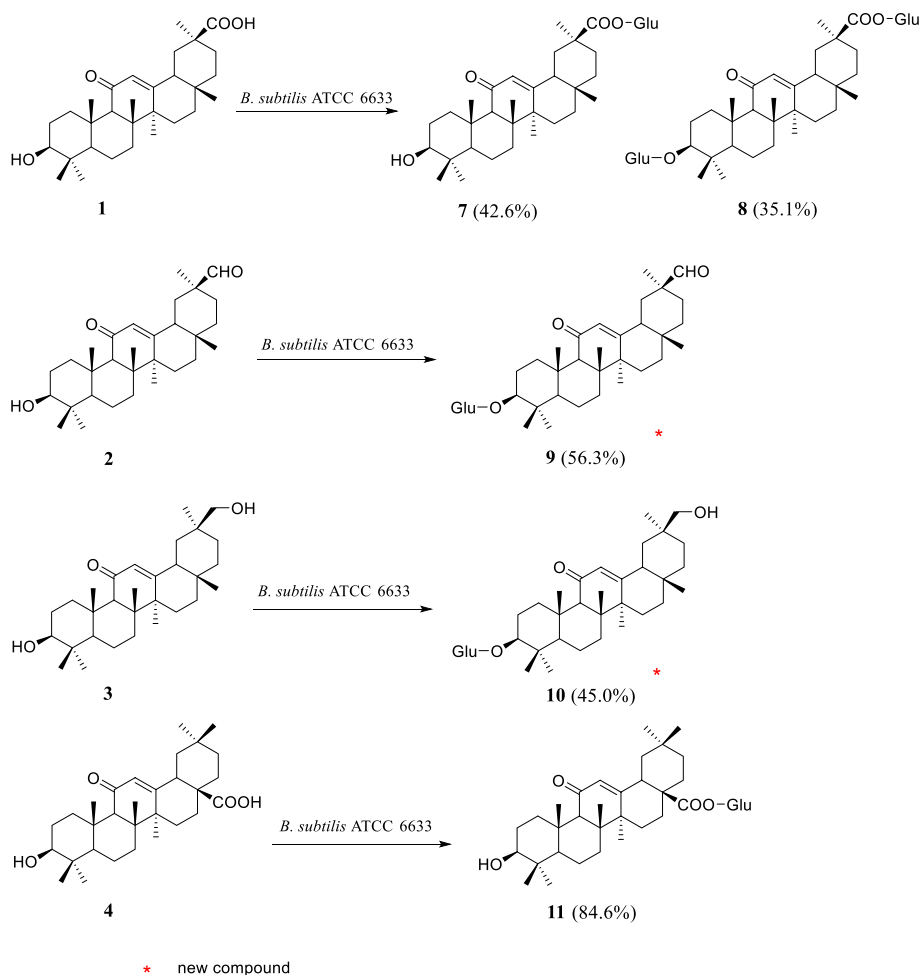


Fig. 3. Biotransformation of 1–4 by *Bacillus subtilis* ATCC 6633.

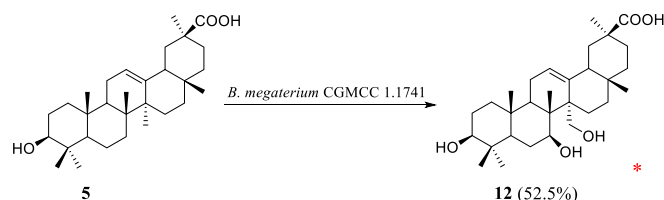


Fig. 4. Biotransformation of 11-deoxyglycyrrhetic acid (5) by *Bacillus megaterium* CGMCC 1.1741.

and showed the long-range correlations with δ 30.7 ppm (C-6), δ 46.9 ppm (C-8), δ 49.7 ppm (C-14) and δ 12.4 ppm (C-26), confirming C-7 of the site of hydroxylation. The new proton signal δ 4.66 ppm had NOE enhancements with δ 1.23 ppm (1H, H-5), indicating that 7-OH should be located in the β -configuration. Another new carbon signal appeared at δ 65.1 ppm was assigned to C-27 since the new proton signal δ 4.40 (d, $J = 12.3$ Hz, 1H), 4.14 (d, $J = 12.3$ Hz, 1H) ppm showed direct correlations with δ 65.1 ppm in HSQC and showed long-range ^1H - ^{13}C correlations with δ 140.1 ppm (C-13), δ 46.9 ppm (C-8), and δ 49.7 ppm (C-14) in HMBC (Fig. 6). Thus, metabolite 12 was identified as: $3\beta,7\beta,27$ -trihydroxy-olean-12-ene-30-oic acid.

Fermentation of 11-deoxyglycyrrhetol (6, 400 mg) by *B. megaterium* yielded a known compound 13 along with six new metabolites 14–19 (Fig. 5).

Compound 13 was obtained as a white powder and the HR-ESI-MS showed a $[\text{M}+\text{H}]^+$ ion at m/z 441.3701 (calcd for $\text{C}_{30}\text{H}_{49}\text{O}_2$, 441.3727). By comparing its ^{13}C NMR with literature, compound 13 was identified as olean-3-oxo-12-en-30-ol, also refers to mupinensisone

which was first discovered in *Euonymus mupinensis*.²³

Compound 14 was obtained as a white powder, possessed a $[\text{M}+\text{H}]^+$ ion at m/z 475.3241 (calcd for $\text{C}_{30}\text{H}_{51}\text{O}_4$, 475.3782), indicating a 32 amu mass increase to that of compound 6. In ^1H NMR spectrum, the new proton signal appeared at δ 4.66 (d, $J = 8.3$ Hz, 1H) ppm, which showed a direct correlation with δ 67.0 ppm in HSQC and showed long-range ^1H - ^{13}C correlations with δ 21.2 ppm (C-27), δ 37.5 ppm (C-10), δ 47.2 ppm (C-8) in HMBC, confirming δ 67.0 ppm was assigned to C-15. The new proton signal δ 4.66 ppm had NOE enhancements with δ 1.33 ppm (s, 3H, H-26), indicating that 15-OH should be located in the α -configuration. According to the similar analysis of the NMR spectrum with 12, the new carbon signal at δ 72.4 ppm could be attributed to C-7. Therefore, compound 14 was identified as olean-12-ene- $3\beta,7\beta,15\alpha,30$ -tetraol.

Compound 15 was obtained as a white powder and HR-ESI-MS showed an $[\text{M}+\text{COOH}]^-$ ion at m/z 535.3617 (calcd for $\text{C}_{30}\text{H}_{50}\text{O}_5\text{COOH}$, 535.3640), which indicated an increment of 48 amu as compared to 6. In the ^{13}C NMR, there were three new carbon signals at δ 72.7 ppm, δ 67.2 ppm, δ 66.8 ppm. The new carbon signal at δ 66.8 ppm was assigned to C-11 since the new proton signal at δ 4.59 (s, 1H) ppm direct correlation with δ 66.8 ppm in HSQC and long-range ^1H - ^{13}C correlations with δ 129.7 (C-12), 148.4 (C-13), 56.8 (C-9), 39.4 (C-10) ppm in HMBC. The signal at δ 4.59 ppm had NOE enhancements with δ 1.29 ppm (s, 3H, H-25), indicating that 11-OH should be located in the α -configuration. By contrast with the spectrum data of 14, the new carbon signals at δ 72.7 ppm and δ 67.2 ppm were attributed to 7β and 15α , respectively. Therefore, metabolite 15 was characterized as olean-12-ene- $3\beta,7\beta,11\alpha,15\alpha,30$ -pentol.

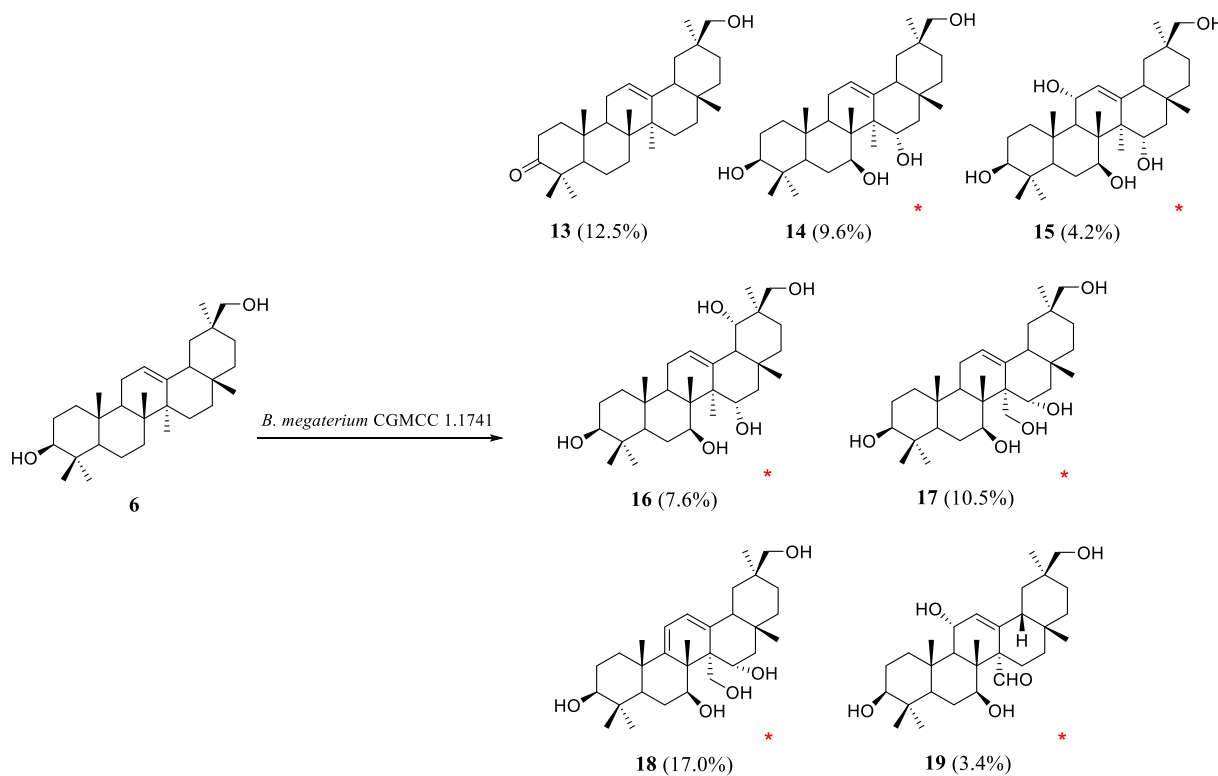


Fig. 5. Biotransformation of 11-deoxyglycyrrhetol (**6**) by *Bacillus megaterium* CGMCC 1.1741.

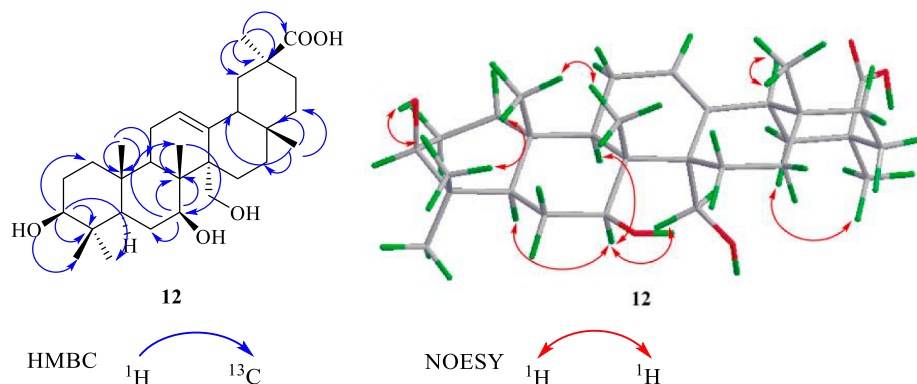


Fig. 6. Key HMBC and NOESY correlations of compound **12**.

Compound **16**, isolated as a white powder, gave an $[M+Cl]^-$ ion at m/z 525.3341 (calcd for $C_{30}H_{50}O_5Cl$, 525.3352). In the ^{13}C NMR, there were three new carbon signals at δ 75.9 ppm, δ 72.5 ppm, δ 67.2 ppm. The new carbon signal at δ 75.9 ppm was assigned to C-19 since the new proton signal at δ 3.88 (m, 1H) direct correlation with δ 75.9 ppm in HSQC and long-range correlations with δ 151.5 (C-13), 39.3 (C-17), 53.4 (C-18) ppm in HMBC. The NOESY spectrum of **16** showed NOE enhancements between δ 3.88 ppm and δ 1.17 ppm (s, 3H, H-28), confirming the 19-OH should be α -configuration (Fig. 6). By contrast with the spectrum data of **14**, the remaining of new carbon signals at δ 72.5 ppm, δ 67.2 ppm were respectively assigned to C-7, C-15. Therefore, metabolite **16** was elucidated as olean-12-ene-3 β ,7 β ,15 α ,19 α ,30-pentol.

Compound **17** was purified as a white powder. The HR-ESI-MS showed a $[M+Na]^+$ ion at m/z 513.3535 (calcd for $C_{30}H_{50}O_5Na$, 513.3505). The ^{13}C NMR spectrum showed the presence of three new carbon signals at δ 73.5, 68.2, 63.4 ppm. In 1H NMR, the new proton signal δ 4.71(1H, d, $J = 12.6$ Hz), 4.39 (1H, d, $J = 12.6$ Hz) ppm showed the direct 1H - ^{13}C correlation with δ 63.4 ppm in HSQC and

showed the long-range correlations with δ 47.8 ppm (C-8), δ 140.65 ppm (C-13), δ 54.3 ppm (C-14), confirming C-27 of the one site of hydroxylation. The remaining of new carbon signals at δ 73.5 ppm, δ 68.2 ppm were very similar to those of compound **14** and respectively assigned to C-7, C-15. Therefore, metabolite **17** was elucidated as olean-12-ene-3 β ,7 β ,15 α ,27,30-pentol.

Compound **18** was purified as a white powder, gave an $[M+Cl]^-$ ion at m/z 523.3178 (calcd for $C_{30}H_{48}O_5Cl$, 523.3196), indicating a 48 amu mass and one degree of unsaturation increase to that of compound **6**. In the ^{13}C NMR spectrum, there had two new olefinic carbons, also quaternary carbon, at δ 157.1, 144.9 ppm been observed. In 1H NMR spectrum, the new proton signal appeared at δ 5.87 (1H, d, $J = 6.1$ Hz) ppm, which showed a direct correlation with δ 125.0 ppm in HSQC and showed long-range 1H - ^{13}C correlations with δ 157.1 ppm, δ 46.3 ppm (C-18), δ 51.5 ppm (C-14) in HMBC, confirming δ 125.0 ppm was assigned to C-12. Another new proton signal appeared at δ 5.72 (1H, d, $J = 6.0$ Hz) ppm, showed a direct correlation with δ 117.8 ppm in HSQC and showed long-range 1H - ^{13}C correlations with δ 144.9 ppm, δ 51.1 ppm (C-8), δ 40.3 ppm (C-10) in HMBC, indicating that δ

Table 1
Inhibition on NO production of compounds 1–19 in LPS-induced RAW264.7 cells.

Compound	IC ₅₀ /μM ^a	Cell viability (%)	Compound	IC ₅₀ /μM	Cell viability (%)
1	NA ^b	4.035 ± 0.31	11	11.05 ± 4.30	82.73 ± 2.40
2	47.17 ± 4.97	89.64 ± 2.38	12	NA	113.75 ± 3.22
3	50.28 ± 7.28	56.57 ± 1.25	13	38.34 ± 0.70	109.80 ± 0.73
4	NA	111.25 ± 2.69	14	NA	119.87 ± 4.61
5	25.61 ± 0.78	83.41 ± 1.55	15	NA	111.84 ± 1.16
6	48.19 ± 2.12	101.89 ± 3.01	16	0.64 ± 0.31	124.59 ± 0.91
7	NA	94.79 ± 2.19	17	0.07 ± 0.87	106.62 ± 2.56
8	NA	120.54 ± 7.55	18	68.87 ± 0.93	129.85 ± 0.72
9	NA	7.33 ± 0.59	19	NA	130.09 ± 1.66
10	NA	1.22 ± 0.06	quercetin ^c	4.53 ± 0.81	106.20 ± 2.20

a: Concentration necessary for 50% inhibition (IC₅₀).

b: NA = no activity; Values are mean ± SD (n = 3).

c: Quercetin was used as a positive control.

117.8 ppm was assigned to C-11. And, the new olefinic carbons δ 157.1 ppm was assigned to C-9 since the proton signal at δ 1.56 (s, 3H, H-26) and δ 1.25 (s, 3H, H-25) ppm showed long-range ¹H–¹³C correlations with it, so another olefinic carbon δ 144.9 ppm should be located at C-13. It is speculated that the new conjugate double bond in C9-C11 and C12-C13 was formed. Compared to the NMR spectra of **12** and **17**, the three new carbon signals at δ 73.6 ppm, δ 69.2 ppm and δ 64.9 ppm in the ¹³C NMR spectrum were assigned to C-7β, C-15α and C-27, respectively. Therefore, the metabolite **18** was identified as: olean-9(11),12(13)-diene-3β,7β,15α,27,30-pentol.

Compound **19**, isolated as a white powder, possessed an [M + Na]⁺ ion at *m/z* 511.3379 (calcd for C₃₀H₄₈O₅Na, 511.3394), indicating one degrees of unsaturation increase to that of compound **6**. In the ¹³C NMR spectrum, three new carbon signals, respectively, displayed at δ 208.2 ppm, δ 74.9 ppm, δ 67.4 ppm. The new carbon signal at δ 208.2 ppm was assigned to C-27 since δ 10.4 ppm (s,1H) showed direct correlations with δ 208.2 ppm in HSQC and showed long-range ¹H–¹³C correlations with δ 139.5 (C-13) ppm, δ 60.7 (C-14) ppm, δ 23.6 (C-15) ppm in HMBC. In contrast to the NMR spectrum of **15**, the remaining new carbon signals at δ 74.9 ppm, δ 67.4 ppm were assigned to C-7 and C-11. Thus, metabolite **19** was determined as 3β,7β,11α,30-tetrahydroxy-olean-12-en-27-aldehyde.

2.3. Anti-inflammatory activity of all the compounds

Compounds 1–19 were submitted to the bioassay of NO inhibitory effect to evaluate possible improvement after structural modifications in LPS-induced RAW 264.7 cells. Discovery of new potential compounds against NO production may be the key to the treatment of inflammation-related diseases, including arthritis, diabetes, metabolic syndrome and tumor.

As shown in Table 1, among all the substrates, two C-11 decarboxylation compounds **5** and **6** possessed a higher inhibitory effect on NO production and lower cytotoxic activity than the corresponding parent compounds. Secondly, glycosylation did not enhance the inhibitory activity of metabolites except for compound **11**. Furthermore, *B. megaterium* catalyzed highly efficient regio-selective oxidation on a non-activated C-H bond of 11-deoxoglycyrrhetol and yielded one known and six new compounds. Among the series of oxidated products, compounds **13** and **18** exhibited moderate NO inhibition effects with IC₅₀ values of 38.34–68.87 μM. Compounds **16** and **17** showed significant inhibitory activity against NO production than the positive control, with IC₅₀ values of 0.64, 0.07 μM, respectively, which is increased by 75 and 688 times compared to the mother compound. A simple structure–activity analysis revealed that compounds **14** and **15** with hydroxyl groups at C-7, C-11 and C-15, exhibited lower NO inhibition activity in contrast to the lead compound **6**. However, compounds **16** and **17**, with hydroxyl groups at C-19 and C-27 respectively, strongly enhanced inhibitory activity over that of quercetin. In

addition, it was found that the inhibitory activity disappeared after the primary alcohol at C-27 was oxidized to aldehyde. As indicated above, the substituent site of hydroxyl group was even crucial to their anti-inflammatory activity.

3. Conclusions

As mentioned in the introduction, glycyrrhizin and especially its biologically active metabolite **GA**, involved in a variety of biological processes, are essential for the treatment of several diseases and disorders. Herein, **GA** and oleanic acid were served as leads in the semi-synthesis of five ring C/E-modified derivatives. Biotransformation of all the six compounds by *B. subtilis* and *B. megaterium* were investigated,

Table 2
¹³C NMR data of compounds 9–19 in C₅D₅N(150 MHz).

Position	9	10	12	14	15	16	17	18	19
1	38.9	39.9	39.4	39.5	41.5	43.0	38.1	38.7	41.6
2	27.0	28.6	28.6	28.9	28.9	29.1	29.0	28.5	28.9
3	89.0	88.9	78.2	78.2	78.2	78.0	78.1	77.7	77.8
4	40.0	40.3	39.5	39.4	39.9	39.8	39.5	39.8	39.9
5	55.7	55.7	53.5	53.1	53.3	53.0	53.1	49.5	53.0
6	18.0	18.0	30.7	29.5	29.6	29.5	29.6	29.8	31.0
7	33.2	33.3	74.3	72.4	72.7	72.5	73.5	73.6	74.9
8	43.8	45.9	46.9	47.2	49.6	49.4	47.8	51.1	51.9
9	62.5	62.4	49.0	48.6	56.8	48.2	48.4	157.1	57.6
10	37.6	37.6	38.1	37.5	39.4	33.2	39.3	40.3	40.0
11	199.8	199.8	24.5	24.4	66.8	21.2	24.8	117.8	67.4
12	129.2	128.9	128.6	124.5	129.7	124.1	129.5	125.0	134.0
13	168.9	170.3	140.1	146.5	148.4	151.5	140.6	144.9	139.5
14	47.3	47.6	49.7	49.6	50.5	50.2	54.3	51.5	60.7
15	24.2	28.6	26.6	67.0	67.2	67.2	68.2	69.2	23.6
16	26.6	23.9	28.5	37.1	37.3	37.1	37.7	38.5	27.9
17	32.4	41.2	39.3	37.9	37.1	39.3	37.1	37.0	36.7
18	48.3	47.6	50.2	48.8	48.0	53.4	48.6	46.3	48.0
19	40.3	44.0	42.9	42.6	42.5	75.9	41.4	42.7	36.2
20	45.9	30.3	44.7	36.5	36.4	36.4	36.5	36.5	39.8
21	28.9	32.8	32.2	30.5	30.4	30.4	30.1	30.3	30.1
22	37.8	36.3	32.8	33.3	33.2	40.0	33.1	33.44	32.6
23	27.0	29.0	29.0	29.0	29.2	28.9	28.9	29.1	28.9
24	17.1	17.4	17.1	17.0	17.0	16.9	17.0	17.0	17.0
25	17.4	17.1	16.8	16.1	17.5	13.8	16.5	26.4	17.8
26	19.1	19.2	12.5	11.4	13.4	29.7	12.7	15.9	13.1
27	27.3	27.3	65.1	21.2	21.6	21.2	63.4	64.9	208.2
28	28.6	28.6	29.2	29.2	29.6	17.7	29.5	29.3	28.8
29	28.7	27.0	29.5	28.5	28.9	28.9	28.6	28.8	28.7
30	206.4	65.8	180.1	65.9	65.8	65.9	66.1	66.1	65.8
Glu-1'	107.3	107.2							
2'	76.2	76.1							
3'	79.2	79.1							
4'	72.6	72.2							
5'	78.7	78.6							
6'	63.4	63.3							

Table 3
¹H NMR data of compounds **12–19** in C₅D₅N(600 MHz).

Position	12	14	15	16	17	18	19
1			2.76 d (13.9)	1.91, m 1.75, m		1.93, m 2.63, t (12.6)	2.93, dd (10.7, 3.3)
2	1.83, m						
3	3.40, dd (11.3,4.8)	3.48, dd (10.2,5.3)	3.57, d (10.7)	3.51, d (7.1)	3.38, d (8.9)	3.42, m	3.45, dd (11.4, 4.7)
4							
5	1.23, m	1.07, m	1.25, m	1.15, m	1.21, m	1.35, m	1.05, m
6	2.06, m						
7	4.66, dd (10.9,4.6)	4.37, d (7.6)	4.41, d (7.4)	4.34, d (8.1)	4.74, m	5.34, m	4.02, dd (10.8,4.4)
8							
9	2.47(m)	1.66, m	2.02, m	2.33, m	2.44, m		2.11, m
10							
11	2.02, m		4.59, s	1.70, m		5.72, d (6.0)	4.79, dd (8.9,2.5)
12		5.46, m	5.81, d (3.4)	5.73, d (3.5)	5.83, m	5.87, d (6.1)	6.18, d (2.8)
13							
14							
15	2.15, m 2.41, m	4.66, d (8.3)	4.71, d (7.5)	4.70, d (9.2)		4.96, d (8.9)	
16	2.18, m		1.33, m			1.39, m	
17							
18	2.60, m	2.25, m	2.2, m	1.93, m	2.34, m	2.34, d (13.8)	2.33, dd (13.4,3.7)
19	1.92, m 2.51, m	1.93, m 1.68, m	1.85, m 1.67, m	3.88, m	1.99, m 1.88, m	1.94, m 1.62, m	
20							
21	1.44, m 2.28, m						
22				2.04, m			
23	1.19, s	1.27, s	1.32, s	1.30, s	1.23, s	1.21, s	1.13, s
24	1.07, s	1.08, s	1.14, s	1.12, s	1.08, s	1.04, s	1.08, s
25	1.03, s	1.03, s	1.29, s	1.36, s	1.02, s	1.25, s	1.30, s
26	1.33, s	1.33, s	1.44, s	1.05, s	1.33, s	1.56, s	1.46, s
27	4.14, d (12.3) 4.40, d (12.3)	1.61, s	1.74, s	1.70, s	4.71, d (12.6) 4.39, d (12.6)	4.62, d (12.0) 4.39, d (12.0)	10.46, s
28	1.06, s	1.02, s	1.05, s	1.17, s	1.06, s	0.98, s	0.99, s
29	1.31, s	1.18, s	1.10, s	1.14, s	1.14, s	1.08, s	0.99, s
30		3.84, dd (11.7, 11.5)	3.87, d (10.3)	3.70, d (10.4)	3.90, d (12.3)	3.77, d (9.8)	3.79, d (10.6)
					3.86, dd (13.1, 9.8)	3.79, dd (18.1, 10.7)	3.79, d (10.6) 3.79, d (10.6)

and nine previously undescribed and four known products were isolated. The results showed *B. subtilis*, holding the robust regio-selective glycosylation ability, could efficiently catalyze aglycones **1–4** to prepare a series of glycosides. Additionally, the culture displayed its preference to the free carboxyl group on the framework than the free hydroxyl group, as indicated in **7** and **11**. *B. megaterium* was observed to be capable of regio- and stereo-selective hydroxylation at unactivated CH₂/CH₃ on the skeleton of **5** and **6**, covering C-7, 11, 15, 19, 27 sites, which greatly expand the chemical diversity of structurally complex PTs. Moreover, the substitution sites at C-19 and C-27 of such PTs was found for the first time by biotransformation, but seen in plant-derived triterpenoids.^{24,25} The anti-inflammatory activity results indicated that metabolite **16**, **17** with hydroxyl groups at C-19, C-27, respectively, significantly inhibited NO release even better than that of positive control quercetin with IC₅₀ values of 0.64, 0.07 μM. In summary, we enriched the structural diversity of PTs by biotransformation and their anti-inflammatory activity at low micromolar concentrations may be worthy of further studies.

4. Materials and methods

4.1. General experimental procedures

All the chemicals and solvents used for extraction and isolation were of analytical grade. NMR spectra were recorded on a Bruker AV-600 spectrometer in C₅D₅N solution, with TMS as the internal standard. The HR-ESI-MS experiments were performed on Agilent 1100 Series MSD Trap mass spectrometer. Preparative reversed-phase HPLC was performed on Agilent 1100 instrument equipped with Alltech 3300 ELSD detector. Separation and purification were performed by column

chromatography on silica gel (200–400 mesh). HPTLC was carried out on precoated silica gel GF254 plates, and the silica gel was bought from Qingdao Marine Chemical Group Co., PR China.

4.2. Microorganism and culture medium

Bacillus subtilis ATCC 6633 were obtained from courtesy of Prof. John P.N. Rosazza of the University of Iowa, USA. *Bacillus megaterium* CGMCC 1.1741 was purchased from China Center of Industrial Culture Collection (CICC). Cultures were cultivated in 50 mL of soybean meal glucose medium by a two-stage procedure held in 250 mL culture flasks. The soybean meal glucose medium contained 20 g glucose, 5 g soybean meal, 5 g yeast extract, 5 g NaCl and 5 g K₂HPO₄ in one-liter distilled water and was adjusted to pH 7.0 with 6 N HCl before being autoclaved at 121 °C for 20 min. GA was purchased from Nanjing Plant Origin Biological Technology Co., Ltd.

4.3. Fermentation, extraction and isolation

Cultures were incubated on a rotary shaker at 28°C and 180 rpm. A 10% inoculum derived from the 24-h-old stage I culture was used to initiate the stage II culture, which was incubated for 24 h, and 1 mL of acetone with 10 mg of the substrates was sequentially added. Cultures were incubated for 4 days and extracted with equal volumes of EtOAc three times. The organic layer was concentrated and isolated on silica gel column chromatography and gradient eluted with CH₂Cl₂/CH₃OH (100:1–2:1, v/v). The samples were spotted on silica gel HPTLC plates, and the results were visualized by spraying with H₂SO₄ (10% in ethanol). According to high-performance thin layer chromatography (HPTLC) analysis, similar fractions were combined and further

subjected to preparative HPLC with CH₃CN/H₂O as the mobile phase. The compounds were isolated at 30%-40% acetonitrile in water and were further characterized by spectrometry.

30-O-β-D-glucopyranosyl glycyrrhaldehyde (**9**): white powder; ¹H NMR and ¹³C NMR (pyridine-d₅), see Tables 2 and 3, respectively; negative HR-ESI-MS *m/z* 651.4124 [M+Cl]⁻ (calcd for C₃₆H₅₆O₈Cl, 651.3669).

3β,7β,27-Trihydroxy-olean-12-ene-30-oic acid (**12**): white solid; ¹H NMR and ¹³C NMR (pyridine-d₅), see Tables 2 and 3, respectively; negative HR-ESI-MS *m/z* 523.3179 [M+Cl]⁻ (calcd for C₃₀H₄₈O₅Cl, 523.3196).

Olean-12-ene-3β,7β,15α,30-tetraol (**14**): white solid; ¹H NMR and ¹³C NMR (pyridine-d₅), see Tables 2 and 3, respectively; positive HR-ESI-MS *m/z* 475.3241 [M+H]⁺ (calcd for C₃₀H₅₁O₄, 475.3782).

Olean-12-ene-3β,7β,11α,15α,30-pentol (**15**): white powder; ¹H NMR and ¹³C NMR (pyridine-d₅), see Tables 2 and 3, respectively; negative HR-ESI-MS *m/z* 535.3617 [M+COOH]⁻ (calcd for C₃₀H₅₀O₅COOH, 535.3640).

Olean-12-ene-3β,7β,15α,19α,30-pentol (**16**): white powder; ¹H NMR and ¹³C NMR (pyridine-d₅), see Tables 2 and 3, respectively; negative HR-ESI-MS *m/z* 525.3341 [M+Cl]⁻ (calcd for C₃₀H₅₀O₅Cl, 525.3352).

Olean-12-ene-3β,7β,15α,27,30-pentol (**17**): white solid; ¹H NMR and ¹³C NMR (pyridine-d₅), see Tables 2 and 3, respectively; positive HR-ESI-MS *m/z* 513.3535 [M+Na]⁺ (calcd for C₃₀H₅₀O₅Na, 513.3550).

Olean-9(11),12(13)-diene-3β,7β,15α,27,30-pentol (**18**): white powder; ¹H NMR and ¹³C NMR (pyridine-d₅), see Tables 2 and 3, respectively; negative HR-ESI-MS *m/z* 523.3178 [M+Cl]⁻ (calcd for C₃₀H₄₈O₅Cl, 523.3196).

3β,7β,11α,30-Tetrahydroxy-olean-12-en-27-aldehyde (**19**): white solid; ¹H NMR and ¹³C NMR (pyridine-d₅), see Tables 2 and 3, respectively; positive HR-ESI-MS *m/z* 511.3379 [M+Na]⁺ (calcd for C₃₀H₄₈O₅Na, 511.3394).

4.4. Cell culture and NO measurement

The macrophage RAW 264.7 cell line was purchased from Peking Union Medical College (PUMC) Cell Bank (Beijing, China) and was cultured in DMEM (Gibco, C11965500BT) added with 10% FBS (Gibco,10099141), penicillin G (100 units/mL) and streptomycin (100 µg/mL) (BI, 03-031-1B) and incubated at 37 °C in 5% CO₂ and 95% humidity atmosphere. Tested compounds were separately dissolved in DMSO (Sigma, D2650) with the final concentration of 50 mM and further diluted to test concentrations (100, 50, 25, 12.5, 6.25, 3.125 µM). The RAW 264.7 cells were added in 96-well culture plates at a density of 7.0 × 10⁴ cells/well and co-cultivated with test compounds 1 h before added with LPS (1.0 µg/mL, Sigma, L2880). After 24 h incubation, NO concentration was measured by Griess reagent kit (Beyotime, S0023).

Declaration of Competing Interest

The authors declare that they have no known competing financial interests or personal relationships that could have appeared to influence the work reported in this paper.

Acknowledgements

This Project was supported by Jiangsu Planned Projects for Postdoctoral Research Funds (Grant No. 2018K085B) and the Fundamental Research Funds for the Central Universities (Grant No. 2632018PY14).

Appendix A. Supplementary material

Supplementary data to this article can be found online at <https://doi.org/10.1016/j.bmc.2020.115465>.

References

- Zhao Y, Lv B, Feng X, Li C. A Perspective on biotransformation and de novo biosynthesis of licorice constituents. *J Agric Food Chem*. 2017;65(51):11147–11156.
- Rizzato G, Scalabrini E, Radaelli M, Capodaglio G, Piccolo O. A new exploration of licorice metabolome. *Food Chem*. 2016;221:959–968.
- Mollica L, Marchis FD, Spitaleri A, et al. Glycyrrhizin binds to high-mobility group box 1 protein and inhibits its cytokine activities. *Chem Biol*. 2007;14(4):431–441.
- Takahashi K, Yoshino T, Maki Y, Ishiuchi KI, Watanabe K. Identification of glycyrrhizin metabolites in humans and of a potential biomarker of licorice-induced pseudoalcoholism: a multi-centre cross-sectional study. *Arch Toxicol*. 2019;93(11):3111–3119.
- Singh H, Kim S, Kang DH, et al. Glycyrrhetic acid as a hepatocyte targeting unit for an anticancer drug delivery system with enhanced cell type selectivity. *Chem Commun*. 2018;54(87):12353–12356.
- Lei Y, Kong Y, Sui H, Feng J, Wang W. Enhanced oral bioavailability of glycyrrhetic acid via nanocrystal formulation. *Drug Deliv Transl Res*. 2016;6(5):1–7.
- Tian Q, Wang XH, Wang W, Zhang CN, Wang P, Yuan Z. Self-assembly and liver targeting of sulfated chitosan nanoparticles functionalized with glycyrrhetic acid. *Nanomed Nanotechnol Biol Med*. 2012;8(6):870–879.
- Inoue H, Kurosu S, Takeuchi T, Mori T, Shibata S. Glycyrrhetic acid derivatives: anti-nociceptive activity of deoxoglycyrrhetol dihemiphthalate and the related compounds. *J Pharm Pharmacol*. 1990;42(3):199–200.
- Kimura M, Kimura I, Muroi M, Nakamura T, Shibata S. Depolarizing effects of glycyrrhizin-derivatives relating to the blend effects with paeoniflorin in mouse diaphragm muscle. *Jpn J Pharmacol*. 1986;41(2):263–265.
- Santos GFD, Lima GDS, Oliveira GPD. New AChE inhibitors from microbial transformation of trachyloban-19-oic acid by *Syncephalastrum racemosum*. *Bioorg Chem*. 2018;79:60–63.
- Syed AS, Huey LT, Sadia S. Microbial-catalyzed biotransformation of multifunctional triterpenoids derived from phytonutrients. *Int J Mol Sci*. 2014;15(7):12027–12060.
- Hernández-Martín A, von Bühler CJ, Tieves F, Fernández S, Ferrero M, Urlacher VB. Whole-cell biotransformation with recombinant cytochrome P450 for the selective oxidation of Grundmann's ketone. *Bioorg Med Chem*. 2014;22(20):5586–5592.
- Zhang C, Xu SH, Ma BL, Wang WW, Yu BY, Zhang J. New derivatives of ursolic acid through the biotransformation by *Bacillus megaterium* CGMCC 1.1741 as inhibitors on nitric oxide production. *Bioorg Med Chem Lett*. 2017;27(11):2575–2578.
- Luo SL, Dang LZ, Zhang KQ, Liang LM, Li GH. Cloning and heterologous expression of UDP-glycosyltransferase genes from *Bacillus subtilis* and its application in the glycosylation of ginsenoside Rh1. *Let Appl Microbiol*. 2015;60(1):72–78.
- Wen XA, Sun HB, Liu J. Naturally occurring pentacyclic triterpenes as inhibitors of glycogen phosphorylase: synthesis, structure-activity relationships, and X-ray crystallographic studies. *J Med Chem*. 2008;51(12):3540–3554.
- Terasawa T, Okada T, Nishino H. Anti-tumor-promoter activity of modified glycyrrhetic acid derivatives. Synthesis and structure-activity relationships. *Eur J Med Chem*. 1992;27(7):689–692.
- Tode T, Uesugi T, Hirai K, Nukaya H, Tsuji K, Ishida H. New 6-O-acetyl isoflavone glycosides from soybeans fermented with *Bacillus subtilis* (natto). I. 6-O-succinylated isoflavone glycosides and their preventive effects on bone loss in ovariectomized rats fed a calcium-deficient diet. *Biol Pharm Bull*. 1999;22(11):1193–1201.
- Su X, Lawrence H, Ganeshapillai D, et al. Novel 18β-glycyrrhetic acid analogues as potent and selective inhibitors of 11β-hydroxysteroid dehydrogenases. *Bioorg Med Chem*. 2004;12(16):4439–4457.
- Shibata S, Takahashi K, Yano S, et al. Chemical modification of glycyrrhetic acid in relation to the biological activities. *Chem Pharmaceut Bull*. 1987;35(5):1910–1918.
- Zhang Y, Li JX, Zhao J, et al. Synthesis and activity of oleanolic acid derivatives, a novel class of inhibitors of osteoclast formation. *Bioorg Med Chem Lett*. 2005;15(6):1629–1632.
- Budaev AS, Mikhailova LR, Spirikhin LV, Makara NS, Zarudii FS, Baltina LA. Synthesis and hypoglycemic activity of 11-deoxoglycyrrhetic acid derivatives. *Chem Nat Compd*. 2016;52(3):441–444.
- Hayashi H, Yamada K, Fukui H, Tabata M. Metabolism of exogenous 18β-glycyrrhetic acid in cultured cells of *Glycyrrhiza glabra*. *Phytochemistry*. 1992;31(8):2724–2733.
- Riaz T, Abbasi MA, Riaz N, et al. Isolation, structure elucidation and antioxidant screening of secondary metabolites from rhynchosia pseudo-cajan. *J Chem Soc Pak*. 2012;34(5):1204–1212.
- Eom HJ, Kang HR, Kim HK, et al. Bioactivity-guided isolation of antioxidant triterpenoids from *Betula platyphylla* var. *japonica* bark. *Bioorg Chem*. 2016;66:97–101.
- Han JH, Zhou W, Li W, Tuan PQ, Myung CS. Pentacyclic triterpenoids from *astilbe rivularis* that enhance glucose uptake via the activation of Akt and Erk1/2 in C2C12 myotubes. *J Nat Prod*. 2015;78(5):1005–1014.